

Supplemental Information

Continuous Reactor for Renewable Methanol

Author names and affiliations

Athanasios A. Tountas¹, Geoffrey A. Ozin², Mohini M. Sain^{1,3}

¹ Department of Chemical Engineering and Applied Chemistry, 200 College St., Toronto, ON, M5S 3E5

² Department of Chemistry, 80 St. George St., Toronto, ON, M5S 3H6

³ Department of Mechanical and Industrial Engineering, 5 King's College Rd., Toronto, ON, M5S 3G8

Corresponding author

G. A. Ozin: g.ozin@utoronto.ca

Recycle Compressor Capital and Operating Cost per MT_{MeOH}

The recycle system block diagram is shown in Fig. S1. We assumed complete condensation and separation of the products water and MeOH from the effluent stream S3. The recycle stream is S5 and combines with the inlet stream S1 (100 mol s^{-1} of 3:1 $H_2:CO_2$). Stream S1 is considered to be already at pressure *via* the H_2 and CO_2 feed compressors (not shown). Water and MeOH are completely condensed out in stream S4.

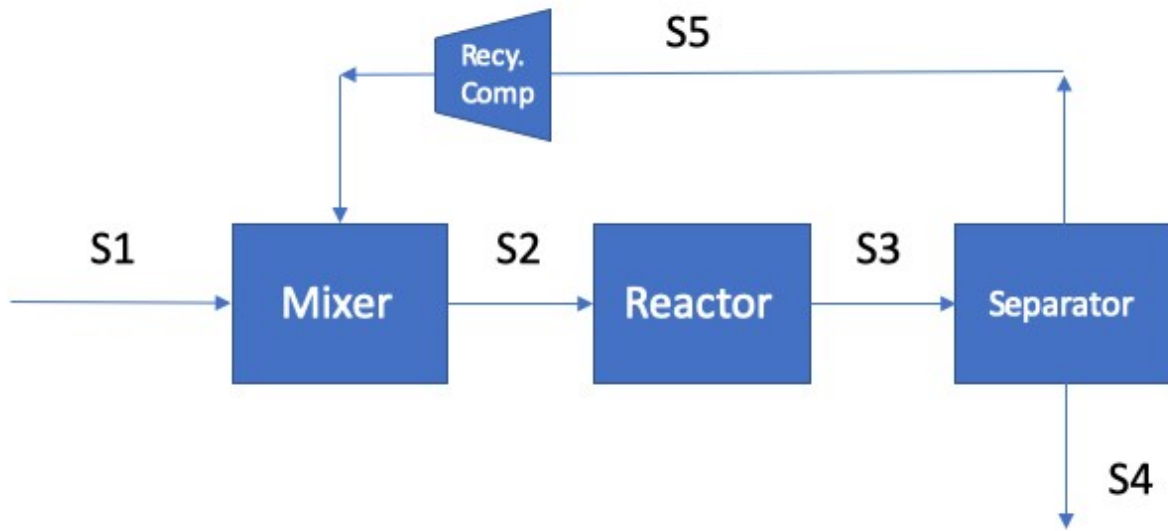


Figure S1: Recycle loop with recycle compressor

The recycle compressor is modeled based on polytropic ($Pv^n = \text{constant}$) operation with an efficiency of 70%. The power requirement can be found either by calculating the outlet temperature (eq. (S1)) or calculated by knowing the starting/ending pressures and starting temperature (eq. (S2)). The gas was assumed to be at 298 K pre-compression.

$$T_2 = T_1 * \left(\frac{P_2}{P_1}\right)^{\frac{(\kappa - 1)}{\kappa}} \quad (S1)$$

$$W_{comp,in} = \frac{nR(T_2 - T_1)}{\kappa - 1} = \frac{nRT_1}{\kappa - 1} \left[\left(\frac{P_2}{P_1} \right)^{\frac{\kappa - 1}{\kappa}} - 1 \right] \quad (S2)$$

Once the power was known, the efficiency was applied (eq. (S3)) and thereafter the cost in US\$ was found by eq. (S4) ¹. The power or P_c is in horsepower (1 hp = 0.746 kW).

$$W_{comp,real} \text{ (or } P_c) = \frac{W_{comp,real}}{\eta_{eff}} \quad (S3)$$

$$C_{compressors} = \exp(7.9661 + 0.8 \ln(P_c)) \quad (S4)$$

The cost of electricity was assumed as US\$ 200 MWh⁻¹. The capital cost was averaged over 10 years of MeOH production (or the plant lifetime), while the operating cost was averaged over one year's production of 23,070 MT_{MeOH} yr⁻¹.

The recycle flow was determined using spreadsheet software. The method assumes a per-pass conversion for CO-rich feed (per-pass equilibrium conversion for CO₂-rich feed) and determines how much recycle is required to achieve complete (100%) conversion of reactants.

Tab. S1 shows how the compressor CAPEX and OPEX compares for CO₂-rich streams (as a function of CO₂ conversion) to CO-rich streams (commercial strategies) at an example pressure of 8 MPa. Also shown are two ideal CO₂-rich scenarios at 1 and 5 MPa that highlight the green benefits of low temperature and the associated higher equilibrium conversion. As can be seen they are on the order of the commercial recycle compressor costs for a classically less productive feed material. The recycle compressor cost per kg_{MeOH} for the commercial process is US\$ 0.095, a reasonable number as from our previous work ² we found the total commercial cost of MeOH on the order of ~ US\$ 0.33 kg_{MeOH}⁻¹.

Table S1: Example comparison of CO₂-rich vs. CO-rich feeds for MeOH production as a function of conversion (%XCO_x). All CO₂-rich cases use a feed of 3:1 H₂:CO₂. The CO-rich cases use a commercial feed of 2.85:29.0:68.15% CO₂:CO:H₂.

Example Set of Criteria	CO ₂ -rich						CO-rich (commercial)		CO ₂ -rich (ideal scenario)	
Per-pass XCO _x %, (Per-pass MeOH yield, %)	10	20	30	50	70	90	45 (20)	63 (33)	30 (8.8)	47 (15.4)
P, MPa, (T, deg C)	8	8	8	8	8	8	8 (250)	8 (250)	1 (125)	5 (175)
Power, kW	19584	8704	5077	2176	933	242	2947	1464	1924	2030
CAPEX, US\$ M	49.4	25.8	16.8	8.5	4.3	1.5	10.9	6.2	7.7	8.1
Outlet MeOH, mol s ⁻¹	25.0	25.0	25.0	25.0	25.0	25.0	33.3	33.3	25.0	25.0
Outlet MeOH, kg s ⁻¹	0.80	0.80	0.80	0.80	0.80	0.80	1.07	1.07	0.80	0.80
Electricity cost, US\$ MWh ⁻¹	200	200	200	200	200	200	200	200	200	200
OPEX, US\$ M	31.3	13.9	8.1	3.5	1.5	0.4	4.7	2.3	3.1	3.2
Plant size, kMt _{MeOH} yr ⁻¹	23.1	23.1	23.1	23.1	23.1	23.1	30.8	30.8	23.1	23.1
OPEX, US\$ Mt _{MeOH} ⁻¹	1358	604	352	151	65	17	153	76	133	141
Total CAPEX + OPEX in US\$ Mt _{MeOH} ⁻¹	1572	716	425	188	83	23	189	96	167	176
Relative to best commercial strategy, %	1638	746	443	196	86	24	197	100	174	183

Testing Criteria: Exclusion of Heat and Mass Transport Limitations

Table S2: Transport property criteria; please see calculations for details of parameters

Equation no.	Criteria	Description	Equation
(S1)	Weisz-Prater ³	Internal or Intraparticle mass transfer	$C_{WP} = \frac{r_{obs} \rho_B R_p^2}{D_e C_{As}} \ll 1$
(S10)	Mears ⁴	External or Interphase mass transfer	$\omega = \frac{r_{obs} \rho_B R_p}{k_c C_{A,b}} \leq \frac{0.15}{n}$
(S14)	Anderson ⁵	Internal or Intraparticle heat transfer	$C_A = \left(\frac{E_{app}}{RT} \right) \left \frac{\Delta H_r r_{obs} \rho_B R_p^2}{\lambda_{eff} T} \right < 0.7!$
(S15)	Mears ⁴	External or Interphase heat transfer	$\chi = \left \frac{\Delta H_r r_{obs} \rho_B R_p E_{app}}{h_p T^2 R} \right < 0.15$

Internal Mass Transfer Limitations

The effect of internal mass transfer limitations can be evaluated by the Weisz-Prater criterion, according to eq. (S5).

$$C_{WP} = \frac{r_{obs} \rho_B R_p^2}{D_e C_{As}} \ll 1 \quad (S5)$$

Where C_{WP} is the Weisz-Prater criterion, r_{obs} is the observed reaction rate per unit of mass of solid catalyst ($\text{mol} \cdot \text{g}^{-1} \cdot \text{hr}^{-1}$), ρ_B is the bulk (apparent) density of the catalyst particles ($\text{g} \cdot \text{m}^{-3}$), R_p is the catalyst particle radius (m), D_e is the effective diffusion coefficient ($\text{m}^2 \cdot \text{hr}^{-1}$) and C_{As} is the concentration of the limiting reactant ($\text{mol} \cdot \text{m}^{-3}$) at the outside of the catalyst surface. In this case CO_2 is the limiting reagent due to the overall 2:1 $\text{H}_2:\text{CO}_2$ stoichiometry when RWGS and CO_2 -to-MeOH proceed equally (feed 3:1 $\text{H}_2:\text{CO}_2$).

The observed rate (r_{obs}) was fixed to the maximum combined MeOH (13.2 mmol·g⁻¹·hr⁻¹) and CO (16.8 mmol·g⁻¹·hr⁻¹) value observed during experimentation. The value of rate and the experimental conditions are reported in **Table S3**.

Table S3. Experimental conditions at which maximum rate was observed

Temperature / K (°C)	Partial pressure of CO ₂ , p_{CO2} / MPa	WHSV / hr ⁻¹	Rate of MeOH & CO production, r_{obs} / mol g ⁻¹ hr ⁻¹
523 (250)	0.195	743	0.030

The bulk catalyst density is calculated assuming it has no porosity (most rigorous case). The as-bought catalyst had an apparent (bulk) density of 1.32 g ml⁻¹ and expected porosity of 40 %. Using (S6),

$$\varepsilon_B = \left(1 - \frac{\rho_B}{\rho_D}\right) * 100 \quad (S6)$$

$$40 = \left(1 - \frac{1.32}{\rho_D}\right) * 100$$

$$\frac{1.32}{\rho_D} = 0.6$$

$$\rho_D = 2.2 \frac{g}{ml}$$

The particle diameter was taken as the average of the sieve sizes (180 to 250 μm). Therefore, the radius was taken to be 107.5 μm.

Estimation of D_e and C_{As} :

Calculation of C_{As}

First approximation is to use the ideal gas law equation to determine the concentration of CO₂ at reaction temperature (T). After rearranging, equation (S7) is obtained.

$$C_{As} = \frac{p_{CO_2}}{R \cdot T} \quad (S7)$$

The calculation is given below for $T = 523.15 \text{ K}$ ($250 \text{ }^\circ\text{C}$):

$$C_{As} = \frac{0.195 \cdot 10^6 \text{ Pa}}{8.3145 \frac{\text{J}}{\text{mol} \cdot \text{K}} \cdot 523.15 \text{ K}} = 44.83 \frac{\text{mol}}{\text{m}^3}$$

Determination of D_e was calculated according to Ortega ⁵

The effective diffusivity (D_e) can be calculated from bulk diffusivity (D_b) and the Knudsen diffusivity (D_{Kn}) values. The latter two depend on the mean velocity (\bar{v}_i) and mean free path (λ_i) of molecules, for species i .

The mean velocity of molecules of species i (\bar{v}_i) ($\text{m}\cdot\text{s}^{-1}$) is given by eq. (S8) ⁵, where, k_B is the Boltzmann constant ($1.38048 \cdot 10^{-23} \text{ J}\cdot\text{K}^{-1}$), m_i is the mass of the molecular species i ($m_i = M_i/N_A$), N_A is Avogadro's number ($6.02283 \cdot 10^{23} \text{ molecules mol}^{-1}$), and R is the ideal gas constant ($8.314 \text{ J}\cdot\text{mol}^{-1}\cdot\text{K}^{-1}$). All constants were taken from ⁶.

$$\bar{v}_i = \left(\frac{8 \cdot k_B \cdot T}{\pi \cdot m_i} \right)^{\frac{1}{2}} = \left(\frac{8 \cdot R \cdot T}{\pi \cdot M_i} \right)^{\frac{1}{2}} \quad (S8)$$

The mean free path (λ_i) (m) is given by eq. (S9) ⁵, where $\sigma_{r,i}$ is the molecular radius of molecule i (for CO₂ $\sigma_r = 3.941 \cdot 10^{-10} \text{ m}$ ⁷), N_i/V is density of molecules i , expressed as molecules/ m^3 ($N_i = n \cdot N_A$) and P is the total pressure.

$$\lambda_i = \frac{1}{\sqrt{2} \cdot \pi \cdot \sigma_{r,i}^2 \cdot (N_i/V)} = \frac{k_B \cdot T}{\sqrt{2} \cdot \pi \cdot \sigma_{r,i}^2 \cdot P} \quad (S9)$$

Calculations are given below at $T = 523.15 \text{ K}$ ($250 \text{ }^\circ\text{C}$):

$$\bar{v}_i = \left(\frac{8 \cdot 8.314 \frac{J}{mol \cdot K} \cdot 523.15 K}{\pi \cdot 0.04401 \frac{kg}{mol}} \right)^{\frac{1}{2}} = 501.7 \frac{m}{s}$$

$$\lambda_i = \frac{1.38048 \cdot 10^{-23} \frac{J}{K} \cdot 523.15 K}{\sqrt{2} \cdot \pi \cdot (3.941 \cdot 10^{-10} m)^2 \cdot 0.78 \cdot 10^6 Pa} = 1.342 \cdot 10^{-8} m$$

Knowing \bar{v}_i and λ_i , the bulk (D_b) and Knudsen (D_{Kn}) diffusivities can be calculated from eq. (S10) and (S11)⁵, respectively. A modification of the original D_{Kn} equation was implemented, so that SI units could directly be used.

$$D_b = \frac{\bar{v}_i \cdot \lambda_i}{3} \quad (S10)$$

$$D_{Kn} = 9.7 \cdot r_{pore} \cdot \sqrt{\frac{T}{10 \cdot M}} \quad (S11)$$

Calculations are shown below at T = 523.15 K (250 °C), for the case when the whole catalyst particle is considered. Since this is an internal mass transfer check, an internal pore diameter needs to be considered. The pore diameter chosen for this calculation is 10 nm (on the order of Cu and ZnO nanoparticle diameters), and the pore radius (r_{pore}) is therefore 5 nm. This size corroborates with experimental data as well⁸.

$$D_b = \frac{501.7 \frac{m}{s} \cdot 1.342 \cdot 10^{-8} m}{3} = 2.244 \cdot 10^{-6} \frac{m^2}{s}$$

$$D_{Kn} = 9.7 \cdot 5 \cdot 10^{-9} m \cdot \sqrt{\frac{523.15 K}{10 \cdot 0.04401 \frac{kg}{mol}}} = 1.672 \cdot 10^{-6} \frac{m^2}{s}$$

These values must be corrected to the ‘effective values’ since diffusion inside catalyst particles occurs in pores of irregular shape, of varying cross-section areas, and only part of the cross-section area perpendicular to the direction of the flux is available. To account for these particle

characteristics, an effective diffusivity for bulk and Knudsen diffusion must be calculated according to eq. (S12)⁵, where ε_p is the pellet porosity (or volume void fraction), $\tilde{\tau}_f$ is the tortuosity factor ($\tilde{\tau}_f = \tilde{\tau}/\sigma_c$), that account for both the tortuosity $\tilde{\tau}$ and the constriction factor σ_c .

$$D_{i,e} = \frac{D \cdot \varepsilon_p}{\tilde{\tau}_f} \quad (\text{S12})$$

The values of porosity and tortuosity factors are taken from Ortega⁵. Tortuosity is defined as the distance a molecule travels between two points divided by the shortest distance between the same two points. The constriction factor accounts for variation in the area that is normal to the diffusion flux⁵. These correspond to a porosity of 0.40 and a tortuosity of 0.725. Therefore, the effective bulk diffusion and the effective Knudsen diffusion at 523.15 K are:

$$D_{b,e} = \frac{D_b \cdot \varepsilon_p}{\tilde{\tau}_f} = \frac{2.244 \cdot 10^{-6} \frac{m^2}{s} \cdot 0.40}{0.725} = 1.238 \cdot 10^{-6} \frac{m^2}{s}$$

$$D_{Kn,e} = \frac{D_{Kn} \cdot \varepsilon_p}{\tilde{\tau}_f} = \frac{1.672 \cdot 10^{-6} \frac{m^2}{s} \cdot 0.40}{0.725} = 9.226 \cdot 10^{-7} \frac{m^2}{s}$$

Finally, the effective diffusivity is calculated with eq. (S13)⁵.

$$D_e = \frac{1}{1/D_{b,e} + 1/D_{Kn,e}} \quad (\text{S13})$$

Exemplary calculation is shown at 523.15 K:

$$D_e = \frac{1}{\frac{1}{1.238 \cdot 10^{-6} \frac{m^2}{s}} + \frac{1}{9.226 \cdot 10^{-7} \frac{m^2}{s}}} = 5.286 \cdot 10^{-7} \frac{m^2}{s}$$

Note that the $D_{b,e}$ assumes only CO₂-in-CO₂ bulk diffusion and not CO₂-in-H₂. Taking the CO₂-in-CO₂ case provides a more rigorous calculation of C_{WP} due to H₂ having smaller size and molar

mass. CO₂ will diffuse more readily in H₂ (larger \bar{v}_i and λ_i) leading to an overall higher CO₂-in-H₂ diffusion coefficient and a smaller calculated coefficient.

Finally, C_{WP} can be calculated using eq. (S1).

$$C_{WP,particle} = \frac{0.030 \frac{mol}{g \cdot hr} \cdot \frac{1 hr}{3600 s} \cdot 2.2E6 \frac{g}{m^3} \cdot (107.5 \cdot 10^{-6} m)^2}{5.286 \cdot 10^{-7} \frac{m^2}{s} \cdot 44.83 \frac{mol}{m^3}} = 0.009 \ll 1$$

External Mass Transfer Limitations

The Mears criterion ⁴ was used to determine the influence of external mass transfer limitations; see eq. (S14).

$$\omega = \frac{r_{obs} \rho_B R_p}{k_c C_{A,b}} \leq \frac{0.15}{n} \quad (S14)$$

Where, r_{obs} is the observed rate of CO₂ conversion in mol·g_{cat}⁻¹·s⁻¹, ρ_B is the density of the catalyst bed in g·m⁻³, R_p is the particle radius in m, n is the order of the reaction (order one (1) for CO₂), k_c is the mass transfer coefficient in m·s⁻¹, and $C_{A,b}$ is the concentration of CO₂ in the bulk phase in mol·m⁻³.

Calculation was done at the experimental condition at which the maximum combined reaction rate was observed. Experimental conditions and data used for calculations are presented in **Table S1**.

Using ideal gas law, the concentration of CO₂ in the bulk phase $C_{A,b}$ is determined from eq. (S15).

$$C_{A,b} = \frac{p_{CO2}}{R \cdot T} \quad (S15)$$

The only term outstanding from the criterion is the mass transfer coefficient (k_c), which can be determined by solving the Frössling correlation ³; see eq. (S16).

$$Sh = \frac{k_c D_p}{D_{b,e}} = 2 + 0.6 \cdot Re_p^{1/2} \cdot Sc^{1/3} \quad (S16)$$

If the particle Reynolds number, Re_p , is less than 800, the correlation simplifies to only the first term. The Re was calculated according to eq. (S17), where, ρ and μ are the density ($\text{kg}\cdot\text{m}^{-3}$) and viscosity ($\text{Pa}\cdot\text{s}$) of the fluid, respectively, and V is the velocity.

$$Re_p = \frac{d_p \cdot V \cdot \rho}{\mu} \quad (S17)$$

Taking the velocity to beat the minimum recycle of 1000 sccm (most rigorous) results in a flow of $0.001 \text{ m}^3 \text{ min}^{-1}$, and a velocity of 0.204 m s^{-1} , with the reactor inner diameter as 10.2 mm. The particle size is known from the previous section. By the ideal gas law, the density of the fluid is assumed to be 17.93 mol m^{-3} at 0.78 MPa. Using the molar mass of the mixture, the density becomes 0.224 kg m^{-3} . Finally, the viscosity is found assuming the gas is 100 % CO_2 (most rigorous) to be a value of $2.551\text{E-}5 \text{ Pa}\cdot\text{s}$ ⁹⁶ (at 523 K or 250 °C at 0.78 MPa). The Re_p is then:

$$Re_p = \frac{(0.000215 \text{ m}) \cdot \left(0.204 \frac{\text{m}}{\text{s}}\right) \cdot \left(0.224 \frac{\text{kg}}{\text{m}^3}\right)}{\left(2.551\text{E-}5 \frac{\text{kg}}{\text{m s}}\right)} = 0.39$$

Therefore, the convective mass transfer coefficient, k_c , with $D_{b,e}$ from the previous section (not including the Knudsen pore diffusion), becomes

$$k_c = \frac{2 \cdot D_{b,e}}{D_p} = \frac{2 \cdot (1.238 \cdot 10^{-6} \frac{\text{m}^2}{\text{s}})}{(0.000215 \text{ m})} = 0.0115 \frac{\text{m}}{\text{s}}$$

Assuming reaction order or 1, the application of the Mears' criterion yields:

$$\omega = \frac{0.03 \frac{\text{mol}}{\text{g} \cdot \text{hr}} \cdot \frac{1 \text{ hr}}{3600 \text{ s}} \cdot 2.2\text{E}6 \frac{\text{g}}{\text{m}^3} \cdot \frac{215}{2} \cdot 10^{-6} \text{ m}}{0.0115 \frac{\text{m}}{\text{s}} \cdot 44.83 \frac{\text{mol}}{\text{m}^3}} = 3.82 \cdot 10^{-3} \leq 0.15$$

Internal Heat Transfer Limitations

Internal heat transfer limitations were evaluated via the Anderson's criterion ⁵, shown in eq. (S18).

$$C_A = \left(\frac{E_{app}}{R \cdot T} \right) \left| \frac{\Delta H_r \cdot r_{obs} \cdot \rho_B \cdot R_p^2}{\lambda_{eff} \cdot T} \right| < 0.75 \quad (S18)$$

All parameters have been defined above, except $\lambda_{p,eff}$, the effective thermal conductivity of the particle ($J \cdot m^{-1} \cdot s^{-1} \cdot K^{-1}$).

For non-metallic substances, Ortega ⁵ has indicated that $\lambda_{p,eff}$ values fall within a narrow distribution, in spite of differences in pore size and void fraction. According to Hill ¹⁰, most $\lambda_{p,eff}$ values fall in the range of $0.16 \text{ W} \cdot \text{m}^{-1} \cdot \text{K}^{-1}$ to $0.64 \text{ W} \cdot \text{m}^{-1} \cdot \text{K}^{-1}$. Taking the low end (the most rigorous case), the internal heat transfer criterion becomes:

$$C_A = \left(\frac{35.1 \cdot 10^3 \frac{J}{mol}}{8.3145 \frac{J}{mol \cdot K} \cdot 523.15 K} \right) \left| \frac{-49.6 \cdot 10^3 \frac{J}{mol} \cdot 8.33 \cdot 10^{-6} \frac{mol}{g \cdot s} \cdot 2.2 \cdot 10^6 \frac{g}{m^3} \cdot (107.5 \cdot 10^{-6} m)^2}{0.16 \frac{W}{m \cdot K} \cdot 523.15 K} \right| < 0.75$$

$$C_A = 0.001 < 0.75$$

External Heat Transfer Limitations

Mears ⁴ developed a criterion for heat transfer resistance of the boundary layer in which the observed rate deviates less than 5 %, resulting in eq. (S19).

$$\chi = \left| \frac{\Delta H_r \cdot r_{obs} \cdot \rho_b \cdot r_p \cdot E_{app}}{h_p \cdot T^2 \cdot R} \right| < 0.15 \quad (S19)$$

Where, ΔH_r is the heat of reaction in $J \cdot \text{mol}^{-1}$, E_{app} is the apparent activation energy of the reaction in $J \cdot \text{mol}^{-1}$, and h_p is the gas to particle heat transfer coefficient in $\text{W} \cdot \text{m}^{-2} \cdot \text{K}^{-1}$. If the criterion is not

met, the generated/consumed heat in the particle does not conduct (dissipate/transfer) fast enough to/from the gas leading to hot/cold spots.

The gas to particle heat transfer coefficient (h_p) was calculated from eq. (S20), a correlation from

$$Nu_{D_p} = \frac{h D_p}{k} = 8.74 + 9.34[6(1 - \varepsilon)]^{0.2} Re_{D_p}^{0.2} Pr^{1/3} \quad (S20)$$

Then, to determine h_p , the Prandtl number must be determined. It is defined by eq. (S21).

$$Pr = \frac{C_p \cdot \mu}{k_f} \quad (S21)$$

Correlations were used to determine the heat capacity at constant pressure C_p and the thermal conductivity of the fluid phase k_f at reaction conditions. The viscosity of the fluid was assumed to be 100 % H₂ (more rigorous as a larger value of h is obtained with CO₂ (2.551E-5 Pa·s)) and is found using first the Lee-Kesler method first for density, and then by the Jossi-Stiel-Thodos Method for viscosity ⁶. The value obtained was 1.323E-5 Pa·s. The heat capacity of H₂ at constant pressure C_p (cal·mol⁻¹·K⁻¹) is given by eq. (S22) ⁶.

$$6.62 + 0.00081T \quad (S22)$$

For a heat capacity value of 14.62 kJ·kg⁻¹·K⁻¹ for 273–2500 K, assuming 100 % H₂ for the gas phase is the most rigorous case (lowest h term) as CO₂ C_p is 22.95 kJ·kg⁻¹·K⁻¹. This correlation assumes the fluid is an ideal gas and the heat capacity is not a function of pressure (C_p ≠ f(P)).

Similarly, the thermal conductivity of the fluid phase k_f (W·m⁻¹·K⁻¹) is determined by eq. (S23) ⁶.

$$k_f = \frac{C_1 \cdot T^{C_2}}{1 + C_3/T + C_4/T^2} \quad (S23)$$

In both cases temperature is in K. The constants C_i are included in Table S4

Table S4. Constants to calculate k_f

Constant	k_f
C1	$2.653 \cdot 10^{-3}$
C2	0.7452
C3	12

The value of k_f for 100 % H₂ is $0.275 \text{ W} \cdot \text{m}^{-1} \cdot \text{K}^{-1}$ which is more rigorous compared to the CO₂ value of $0.0346 \text{ W} \cdot \text{m}^{-1} \cdot \text{K}^{-1}$ at 523 K. The porosity is taken as 0.4 and the Re from the previous section (most rigorous). At reaction conditions, it was found that Pr is 0.703. Then, the particle heat transfer coefficient h_p is $22.54 \text{ kW} \cdot \text{m}^{-2} \cdot \text{K}^{-1}$. The application of the Mears' criterion for heat transfer between the particle and the bulk phase yields:

$$\chi = \left| \frac{-49.6 \cdot 10^3 \frac{J}{mol} \cdot 8.33 \cdot 10^{-6} \frac{mol}{g \cdot s} \cdot 2.2 \cdot 10^6 \frac{g}{m^3} \cdot 107.5 \cdot 10^{-6} m \cdot 35.1 \cdot 10^3 \frac{J}{mol}}{22.54 \cdot 10^3 \frac{W}{m^2 \cdot K} \cdot (523.15 K)^2 \cdot 8.3145 \frac{J}{mol \cdot K}} \right| < 0.15$$

$$\chi = 6.7 \cdot 10^{-5} < 0.15$$

Table S5: Transport limitation criteria check results

Equation no.	Criteria name	Value to satisfy criteria	Result from this study
(S5)	Weisz-Prater ³	$C_{WP} \ll 1$	0.009
(S14)	Mears ⁴	$\omega \leq 0.15$	0.0038
(S18)	Anderson ⁵	$C_A < 0.75$	0.001
(S19)	Mears ⁴	$\chi < 0.15$	6.7E-5

Experimental Data for Results and Discussion

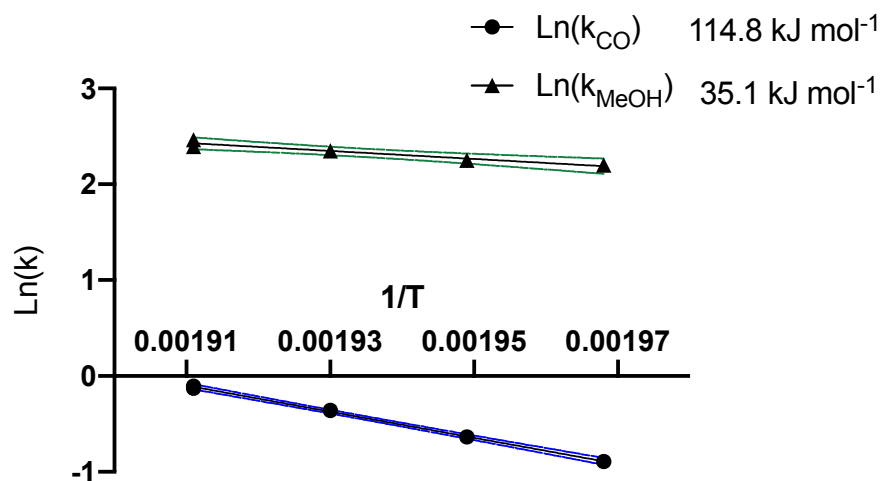


Figure S2: Activation energy for range 508–523 K (235–250 °C) in 5 °C increments, with 95 % confidence intervals

Table S6: Comparison of E_A 's to literature with calculated error

Prod.	#	kJ mol^{-1}	Reaction	Literature Ref.
CO	1	94.8	RWGS	Froment, 1996 ¹²
	2	104.7	RWGS	Skrzypek, 1991 ¹³
	3	123.4 ± 1.6	RWGS	Graaf, 1988 ¹⁴
	4	113.4	RWGS	Kubota, 2001 ¹⁵
	5	94.9	RWGS	Model Graaf ¹⁴
	-	106.2	RWGS	Avg. Lit 1-5
	-	114.8 / 8.0	RWGS	Exp. Run / Error (%)
MeOH	1	36.7	CO ₂ -to-MeOH	Froment, 1996 ¹²
	2	65.2 ± 0.2	CO ₂ -to-MeOH	Graaf, 1988 ¹⁴
	3	32.7	CO ₂ -to-MeOH	Kubota, 2001 ¹⁵
	4	36.2	CO ₂ -to-MeOH	Model Graaf ¹⁴
	5	109.9 ± 0.2	CO-to-MeOH	Graaf, 1988 ¹⁴

-	35.2	CO ₂ -to-MeOH	Avg. Lit 1, 3, 4
-	35.1 / 0.1	CO ₂ -to-MeOH	Exp. Run / Error (%)

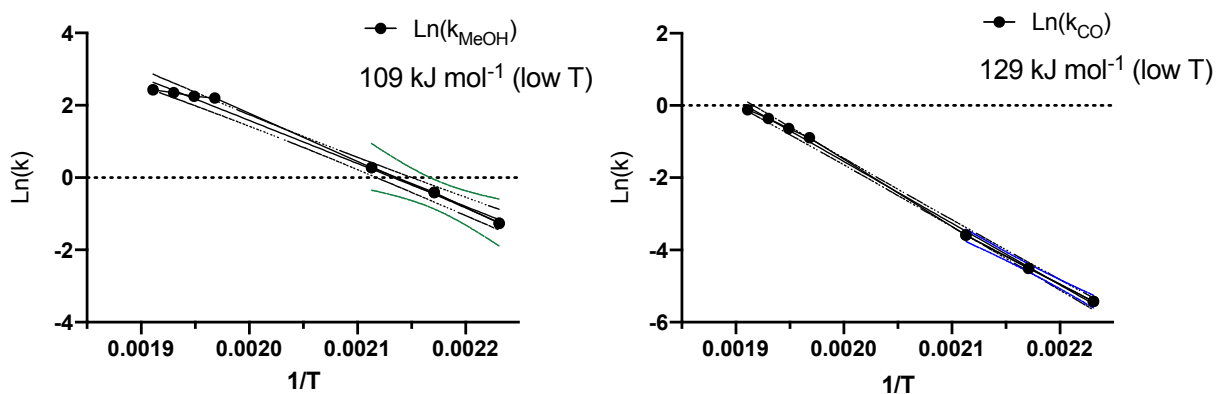


Figure S3: Activation energy change for MeOH (left) showing a deviation from low to high temperature ranges, and for CO (right) staying relatively identical in both temperature ranges

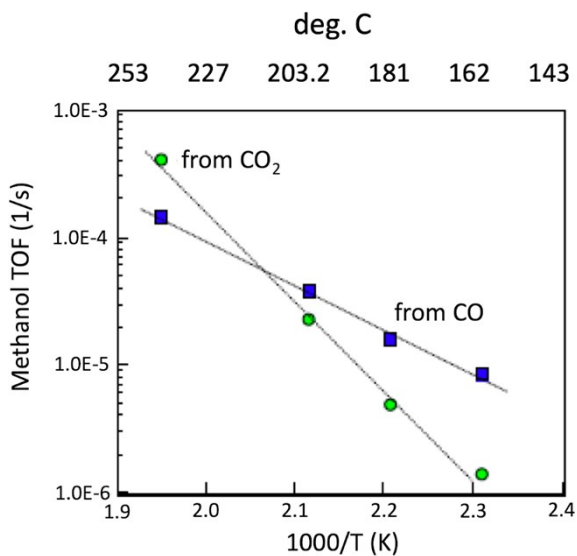


Figure S4: Rates of MeOH production as turnover frequencies (TOFs) from CO (squares) and CO₂ (circles). Conditions: Cu/SiO₂, 6 bar total pressure ¹³CO/CO₂/D₂ = 1:1:6, total flow 10 sccm

Table S7: Literature reference for low-temperature CO₂ and CO-to-MeOH activation energies atP = 6 bar ¹⁶

Component	$E_A / kJ mol^{-1}$
CO ₂	133
CO	66

Table S8: Estimate of the average E_A from 0.5:0.5 CO:CO₂ and 0:1 CO:CO₂ contribution ¹⁶

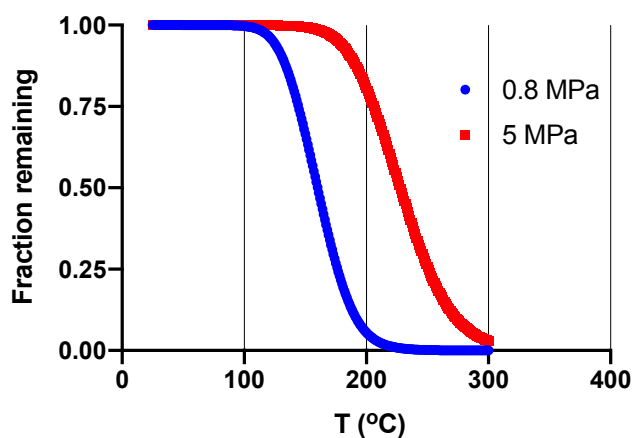
T / K (°C)	435 (161.8)	454 (181)	476.4 (203.2)
MeOH TOF from CO / s ⁻¹	8.10E-06	1.07E-05	3.90E-05
MeOH TOF from CO ₂ / s ⁻¹	1.02E-06	5.00E-06	2.10E-05
% CO-to-MeOH / %	89	68	65
% CO ₂ -to-MeOH / %	11	32	35
E_A if 0.5:0.5 feed CO:CO ₂ / kJ mol ⁻¹	73.5	87.3	89.5
% CO-to-MeOH / %		0	
% CO ₂ -to-MeOH / %		100	
E_A if 0:1 feed CO:CO ₂ / kJ mol ⁻¹		133.0	
E_A avg 0.5:0.5 & 0:1 / kJ mol ⁻¹	103.2	110.2	111.2

Table S9: Activation energies - low temperature, ~ 0.78 MPa

Source	MeOH	CO
E_A this exp. / $kJ\ mol^{-1}$	109	129
E_A lit. / $kJ\ mol^{-1}$	103–111 (low T)	106.5
Error w. lit / %	-1.8–5.8	21

Table S10: Graaf¹⁴ model comparison

P / MPa	T / K ($^{\circ}C$)	S_{MEOH} model / %	ΔS_{MEOH} model / %	$\Sigma \Delta S_{MEOH}$ model / %	S_{MEOH} exp. / %	ΔS_{MEOH} exp. / %	$\Sigma \Delta S_{MEOH}$ exp. / %
0.78	508 (235)	58.1	0	0	56.9	0.0	0
0.78	513 (240)	54.8	-3.3	-3.3	51.9	-5.0	-5.0
0.78	518 (245)	51.5	-3.3	-6.6	47.4	-4.5	-9.5
0.78	523 (250)	48.2	-3.3	-9.9	43.4	-4.0	-13.5

**Figure S5:** Nickel carbonyl equilibrium decomposition temperature

REFERENCES

- 1 M. J. Bos, S. R. A. Kersten and D. W. F. Brilman, *Appl. Energy*, 2020, **264**, 1–11.
- 2 A. A. Tountas, X. Peng, A. V. Tavasoli, P. N. Duchesne, T. L. Dingle, Y. Dong, L. Hurtado, A. Mohan, W. Sun, U. Ulmer, L. Wang, T. E. Wood, C. T. Maravelias, M. M. Sain and G. A. Ozin, *Adv. Sci.*, 2019, **6**, 1–52.
- 3 H. S. Fogler, *Elements of Chemical Reaction Engineering*, 2006.
- 4 D. E. Mears, *Ind. Eng. Chem. Process Des. Dev.*, 1971, **10**, 541–547.
- 5 C. Ortega, M. Rezaei, V. Hessel and G. Kolb, *Chem. Eng. J.*, 2018, **347**, 741–753.
- 6 B. E. Poling, G. H. Thomson, D. G. Friend, R. L. Rowley, C. Engineering and W. V. Wilding, in *Perry's Chemical Engineering Handbook*, McGraw-Hill Professional Publishing, 8th Ed., 2008, pp. 2–88.
- 7 R. A. Svehla, *Estimated Viscosities and Thermal Conductivities of Gases at High Temperatures*, 1962.
- 8 D. Previtali, M. Longhi, F. Galli, A. Di Michele, F. Manenti, M. Signoretto, F. Menegazzo and C. Pirola, *Fuel*, 2020, **274**, 117804.
- 9 M. L. Huber and A. H. Harvey, in *CRC Handbook of Chemistry and Physics*, CRC-Press, Boca Raton, FL, 92nd Ed., 2010, pp. 229–230.
- 10 T. W. R. C. G. Hill, *Introduction to Chemical Engineering Kinetics and Reactor Design*, John Wiley & Sons Inc., 2nd Ed., 2014.
- 11 E. C. Nsofor and G. A. Adebisi, *Exp. Therm. Fluid Sci.*, 2001, **24**, 1–9.
- 12 K. M. Vanden Bussche and G. F. Froment, *J. Catal.*, 1996, **10**, 1–10.
- 13 J. Skrzypek, M. Lachowska and H. Moroz, *Chem. Eng. Sci.*, 1991, **46**, 2809–2813.
- 14 H. Graaf and E. J. Stamhuis, *Chem. Eng. Sci.*, 1988, **43**, 3185–3195.

- 15 M. Kubota, T., Hayakawa, I., Mabuse, H., Mori, K., Ushikoshi, K., Watanabe, T., Saito, *Appl. Organomet. Chem.*, 2001, **15**, 121–126.
- 16 Y. Yang, C. A. Mims, D. H. Mei, C. H. F. Peden and C. T. Campbell, *J. Catal.*, 2013, **298**, 10–17.